Constraints on the temperature-density relation of the intergalactic medium with non-negligible absorber spatial structure

Constraints on the temperature-density relation of the intergalactic medium with non-negligible absorber spatial structure

K N Telikova, P S Shternin and S A Balashev
Ioffe Institute, 26 Politeknicheskaya st., St. Petersburg, 194021, Russia
E-mail: telikova.astro@mail.ioffe.ru

Abstract. We investigate evolution of physical parameters of the intergalactic medium using an analysis of Lyα forest lines detected towards distant quasars. We used the enlarged sample of 98 quasars obtained with Keck/HIRES and VLT/UVES. We show that taking into account a finite spatial size of absorbers, regulated by pressure smoothing, significantly affects the inferred thermal parameters of the intergalactic gas, such as the hydrogen photoionization rate and parameters of the temperature-density relation. Using Bayesian framework we constrained for the first time the scale parameter between the Jeans length and characteristic size of the absorbers. We also discuss limitations of the method based on the analysis of the minimal broadening of Lyα lines, which stem from the patchy nature of He II reionization.

1. Introduction

High-resolution spectroscopy of Lyα forest lines allows one to probe the thermal evolution of the intergalactic medium (IGM) in a wide redshift range, particularly the reionization history of the IGM, which took place at redshifts $z \gtrsim 3$. The temperature-density relation of the IGM contains key information about the reionization scenarios and after the H I reionization (at $z \lesssim 6$), follows a power law [1]:

$$T = T_0 \, \Delta^{\gamma - 1}, \tag{1}$$

where Δ is a density in the units of the mean density $\bar{\rho}$ of the Universe, T is a temperature at a density Δ and $T_0 \equiv T(\Delta = 1)$. The simple form of a single power law in eq (1) can be derived analytically [1]. It stays put in the full hydrodynamic simulations, although, even under the assumption of the uniform He II reionization, it shows some dispersion, which increases with increasing density [1].

One of the widely used methods to probe the evolution of eq (1) with redshift is the analysis of the minimal broadening of the Lyα forest lines in quasar spectra [2–5]. Within the standard approach the minimal broadening of these lines is attributed to the pure thermal broadening due to thermal motions of H I atoms in the absorbing cloud. However, neglect of the absorbers spatial structure may lead to additional uncertainties in the inferred parameters of the temperature-density relation [6–8]. It turns out that a finite extent of IGM filaments increases the minimal broadening of the absorption lines due to the Hubble expansion of the filaments themselves (the so-called Jeans smoothing).

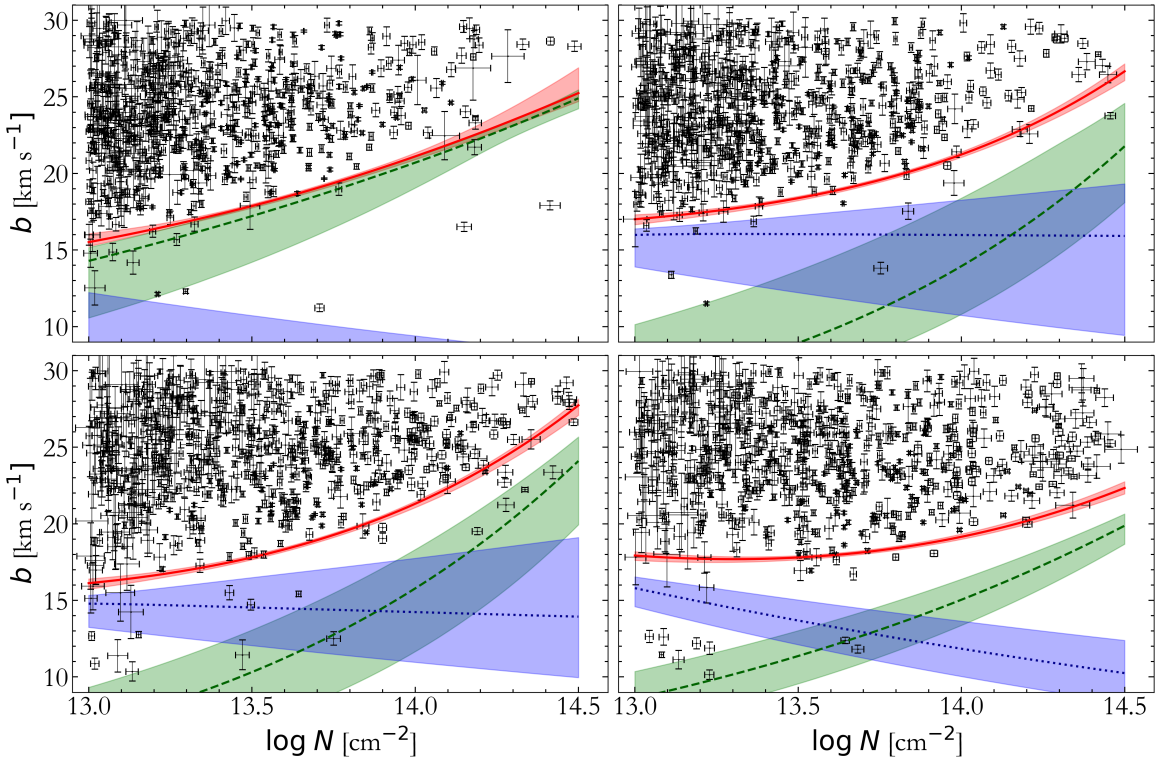

Figure 1. (N, b) distributions of Lyα lines in four redshift bins with mean redshifts 2.2 (upper left), 2.5 (upper right), 2.8 (bottom left) and 3.3 (bottom right). Error crosses indicate the measured sample of the Lyα lines from 98 high-resolution quasar spectra. Solid red curves show the median lower envelope (with corresponding 68 per cent credible intervals shown by red areas) of the obtained (N, b) distributions. Green dashed and blue dotted curves show the contributions of the thermal broadening and the Hubble broadening (with corresponding 68 per cent credible intervals shown by green and blue areas, respectively).

2. Data and method

In our previous study [9] we presented a method to constrain the parameters T_0 and γ of eq (1) by fitting the observed joint distribution of column densities N and Doppler parameters b of Lyα forest lines with the model probability density function. In [9] we assumed purely thermal nature of the lower envelope of the (N, b) distribution and employed 47 quasar spectra from KODIAQ[1] [10] obtained on the Keck telescope. Here we doubled the quasar sample by adding 51 spectra from SQUAD[2] [11] obtained on VLT. As a result, our sample contains 98 high-resolution ($R \sim 36000 - 72000$) and high continuum-to-noise ratio ($C/N \sim 20 - 250$) spectra.

We used the original fitting procedure (see [9, 12, 13]) to obtain a sample of Lyα forest lines in the redshift range $z \sim 1.6 - 4.3$. After the metal line rejection procedure (see [9] for details), the final (N, b) sample contains 2670 lines in total (in comparison with 1503 lines used in [9]). For the further analysis we extend our study [9] taking into account the Hubble broadening due to a non-negligible spatial extent of the absorber. According to [7, 8, 14], the lower (N, b) envelope

[1] Keck Observatory Database of Ionized Absorption toward Quasars
[2] The UVES Spectral Quasar Absorption Database

position $b_{\rm min}(N)$ contains two contributions:

$$b_{\rm min}^2 = \frac{2k_{\rm B}T}{m} + f_{\rm J}^2 \left(\frac{\lambda_{\rm J} H(z)}{2\pi} \right)^2, \quad (2)$$

where $k_{\rm B}$ is the Boltzmann constant, m is the hydrogen atom mass, $\lambda_{\rm J}$ is the Jeans length (which depends on other parameters such as T, Δ etc.) and $H(z)$ is the Hubble parameter. The first term in eq (2) corresponds to the thermal broadening, which dominates at relatively high $\Delta > 1$, and the second one is the broadening due to the Jeans smoothing, which dominates at low Δ. The parameter $f_{\rm J}$ in eq (2) is the scale parameter, which relates the Jeans length and the characteristic size of the IGM filament [7]. Notice that the parameter $f_{\rm J}$ indirectly affects the thermal broadening term in eq (2) through the conversion relation between the column density N and Δ (e.g., [7]). This also means that the second term in eq (2) can not be omitted in the consistent model.

Using the Bayesian framework with the affine Markov Chain Monte Carlo (MCMC) sampler `emcee` [15], we obtained posterior distributions of the parameters of our model. The model contains seven parameters: temperature-density relation parameters γ and T_0, hydrogen photoionization rate Γ, the scale parameter $f_{\rm J}$ and three nuisance parameters. Two nuisance parameters describe the lines' distribution over N and b and the third nuisance parameter describes the fraction of the outliers, see [9] for details. Since the (N, b) distribution depends on the specific combination of T_0 and Γ, as an additional constraint we use the measurements of the Lyα forest effective optical depth from [16] as we did in [9, 14].[3]

During the calculations we assumed a standard ΛCDM cosmology with matter, dark energy and baryon density parameters $\Omega_m = 0.28$, $\Omega_\Lambda = 0.72$ and $\Omega_b = 0.046$, respectively, and the Hubble constant $H_0 = 70$ km s^{-1} Mpc^{-1} [17].

3. Results and discussion

Following [14], we split our data sample into four redshift bins with mean redshifts 2.2, 2.5, 2.8 and 3.3, containing approximately the same number of lines. The respective (N, b) distributions are shown in four panels in figure 1. In figure 1 by the red solid curves enclosed by the corresponded 68 per cent credible intervals we show the minimal broadening $b_{\rm min}(N)$. Green and blue shaded areas show 68 per cent credible intervals corresponding to the thermal and Hubble broadening contributions to $b_{\rm min}$ at each $\log N$, respectively. As seen in figure 1, the minimal broadening is affected by the Jeans smoothing within the whole analysed range of the column densities. This means that neglect of the Jeans smoothing and assumption of the fixed scale factor $f_{\rm J}$[4] can dramatically change the derived parameters of the thermal state of the gas. In figure 2 we show inferred T_0, $f_{\rm J}$ and $\Gamma_{-12} \equiv \Gamma/(10^{-12}\ {\rm s}^{-1})$ in four redshift bins. The temperature estimations in all redshift bins are in agreement with the simulations and semi-analytical models that do not include the He II reionization. However, there is a significant correlation of the temperature-density relation parameters with Γ and $f_{\rm J}$ accompanied by complex shapes of the 2D posterior distributions (see figure 3). Although we match the observed effective optical depth quite well, the obtained $\Gamma_{-12} \sim 1.5$ is relatively high in comparison with measurements and models from literature, particularly for $z \sim 2.5 - 3$ (see, e.g. [24]). Unfortunately, available calculations of the hydrogen photoionization rate are inextricably linked with the assumed IGM temperature [22] (in case of the Lyα forest opacity measurements) or with the ionizing background parameters [26], and cannot be used as independent priors in our studies for the

[3] Unfortunately, in our previous work [14] this constraint was not taken into account properly. Therefore here we do not compare our results with [14] which additionally were obtained with two times smaller sample.

[4] Notice that $f_{\rm J} = 1$ was assumed in most of the previous studies, see, however, [25].

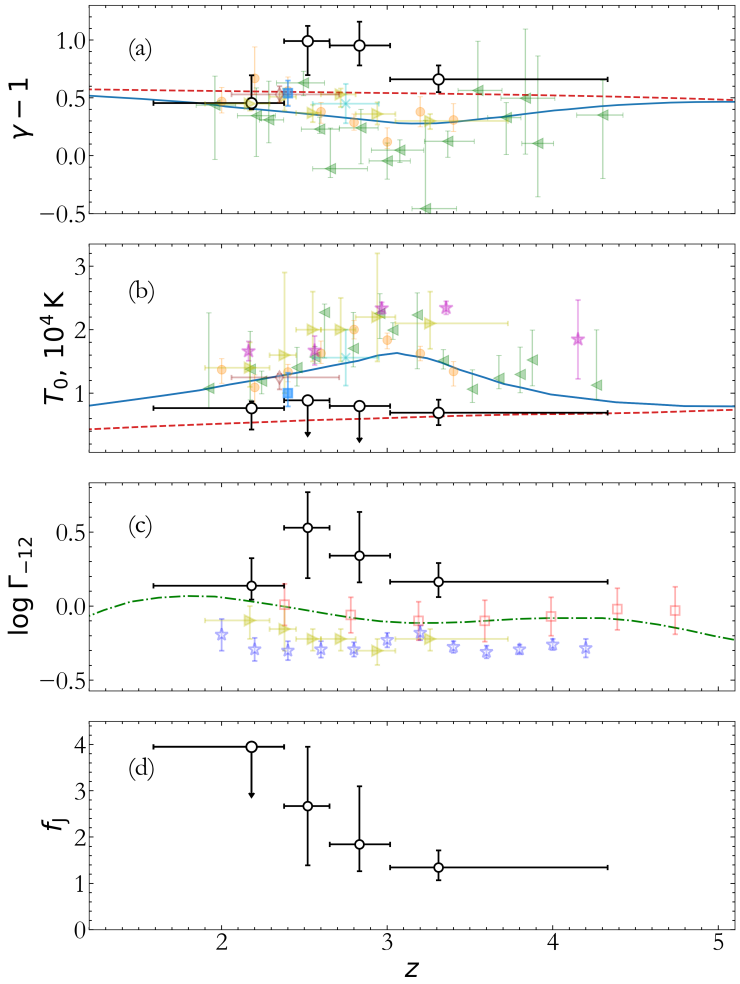

Figure 2. $\gamma - 1$ (a), T_0 (b), Γ_{-12} (c) and f_J (d) as functions of the redshift. Our results are shown by black open circles. Point estimations and upper limits correspond to 0.5 and 0.95 percentiles, respectively. Blue solid and red dashed curves correspond to two different scenarios of the reionization from [18]: with and without accounting for the He II reionization, respectively. We also show measurements of T_0 from [3] (green left triangles), [19] (light-blue filled squares), [5] (yellow filled circles), [20] (cyan crosses), [12] (brown diamonds), [21] (magenta stars), [9] (yellow right triangles) and of Γ_{-12} from [22] (blue open stars, $\gamma - 1 = 0.63$), [23] (red open squares, $\gamma - 1 = 0.40$) and [9] (yellow triangles, γ was a free parameter). The model Γ_{-12} from [24] is shown by green dash-dotted curve.

measurements of the former. Further restrictions on the ionizing background parameters or/and independent constrains on the IGM filaments physical size hopefully will improve this situation.

For models with flat $\Gamma(z)$ and $f_J(z)$ dependencies, the $T_0(z)$ dependence is found to have a peak at the redshifts which correspond to the He II reionization. The amplitude of this peak is highly sensitive to the ionizing background radiation parameters. Possible explanation of such apparent discrepancy of our results with the predictions of simulations, which take into account He II reionization at $z \sim 3$, can lie in the inhomogeneous nature of IGM reionization. Indeed, the recently proposed semi-analytical model, which captures patchy He II reionization (as well as Jeans smoothing) [27], shows that the formation of ionized He III bubbles around strong ionizing radiation sources leads to a more complex picture, where different IGM regions obey diverse temperature-density power laws. In this case until the He III bubbles are significantly overlapped, the low boundary of (N, b) distribution is associated with regions that still are still awaiting He II reionization, and thus are characterised by lower temperatures than ionized ones (see figure 4 in [27]). In principle, the patchy reionization probably does not affect the temperature of IGM, averaged over the sightlines, too dramatically. However, the model presented here as well as similar previous measurements, based on the finding of the exact low boundary of (N, b) distribution, may be not sensitive to regions undergoing He II reionization. Therefore such methods may be inappropriate to catch the He II reionization at least without calibrations with accounting for patchy reionization simulations.

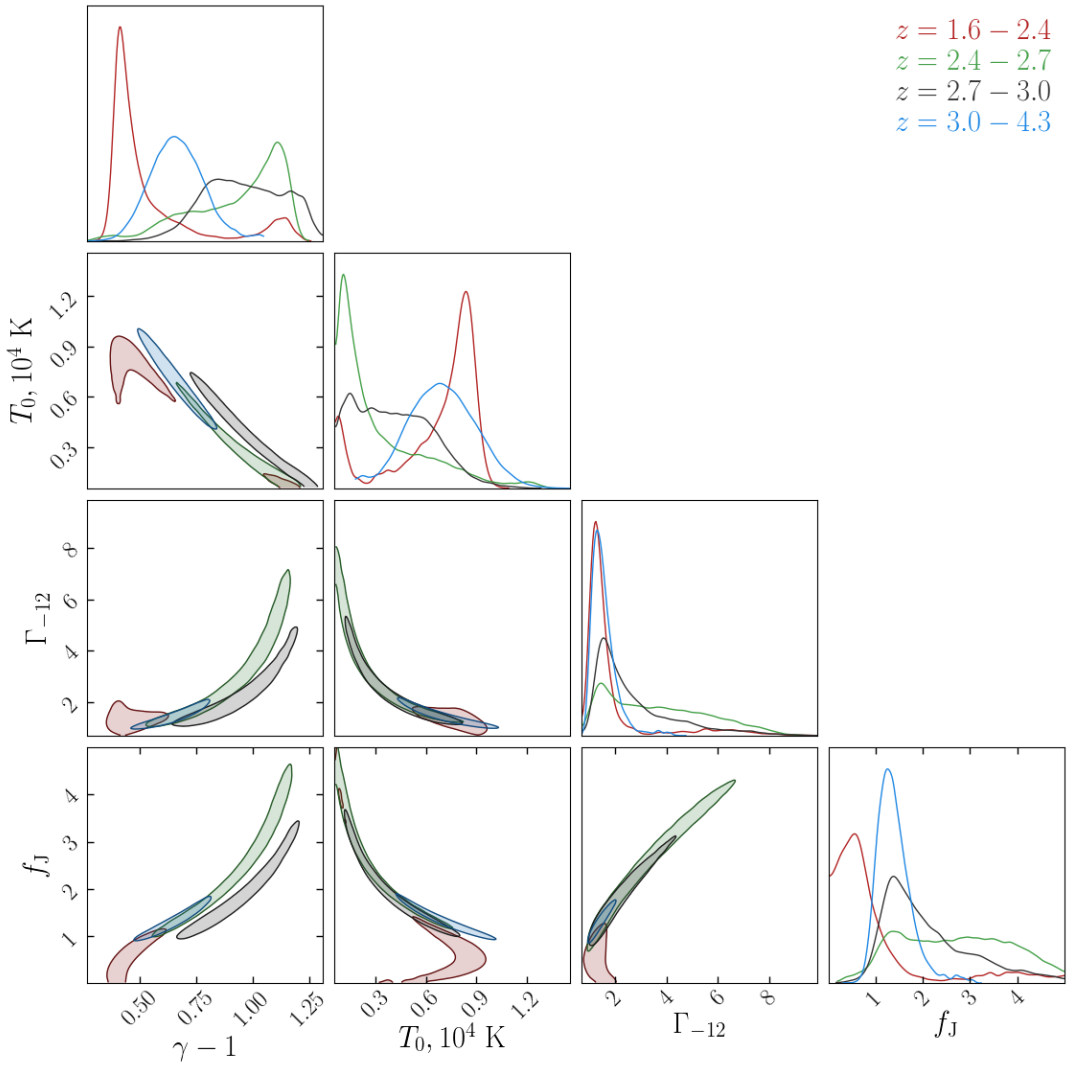

Figure 3. Posterior distributions of temperature-density relation parameters $\gamma - 1$ and T_0, hydrogen photoionization rate Γ_{-12} and scale factor f_J for four redshift bins. 2D distributions are represented by the 68 per cent highest posterior density credible regions.

Acknowledgments
This work is supported by the Foundation for the Advancement of Theoretical Physics and Mathematics "BASIS".

References
[1] Hui L and Gnedin N Y 1997 *MNRAS* **292** 27–42
[2] Schaye J, Theuns T, Leonard A and Efstathiou G 1999 *MNRAS* **310** 57–70
[3] Schaye J, Theuns T, Rauch M, Efstathiou G and Sargent W L W 2000 *MNRAS* **318** 817–26
[4] Rudie G C, Steidel C C and Pettini M 2012 *Astroph. J. Lett.* **757** L30
[5] Hiss H, Walther M, Hennawi J F, Oñorbe J, O'Meara J M, Rorai A and Lukić Z 2018 *Astroph. J.* **865** 42
[6] Hui L, Gnedin N Y and Zhang Y 1997 *Astroph. J.* **486** 599–622
[7] Garzilli A, Theuns T and Schaye J 2015 *MNRAS* **450** 1465–76

[8] Garzilli A, Theuns T and Schaye J 2020 *MNRAS* **492** 2193–2207
[9] Telikova K N, Shternin P S and Balashev S A 2019 *Astroph. J.* **887** 205
[10] O'Meara J M, Lehner N, Howk J C, Prochaska J X, Fox A J, Peeples M S, Tumlinson J and O'Shea B W 2017 *Astron. J.* **154** 114
[11] Murphy M T, Kacprzak G G, Savorgnan G A D and Carswell R F 2019 *MNRAS* **482** 3458–3479
[12] Telikova K N, Balashev S A and Shternin P S 2018 *Journal of Physics: Conference Series* **1038** 012015
[13] Telikova K N, Balashev S A and Shternin P S 2018 *Journal of Physics: Conference Series* **1135** 012010
[14] Telikova K N, Balashev S A and Shternin P S 2019 *Journal of Physics: Conference Series* **1400** 022024
[15] Foreman-Mackey D, Hogg D W, Lang D and Goodman J 2013 *Pub. Astron. Soc. Pacific* **125** 306
[16] Faucher-Giguère C A, Prochaska J X, Lidz A, Hernquist L and Zaldarriaga M 2008 *Astroph. J.* **681** 831–55
[17] Hinshaw G *et al.* 2013 *Astroph. J. Suppl.* **208** 19
[18] Upton Sanderbeck P R, D'Aloisio A and McQuinn M J 2016 *MNRAS* **460** 1885–97
[19] Bolton J S, Becker G D, Haehnelt M G and Viel M 2014 *MNRAS* **438** 2499–507
[20] Rorai A, Carswell R F, Haehnelt M G, Becker G D, Bolton J S and Murphy M T 2018 *MNRAS* **474** 2871–83
[21] Lidz A, Faucher-Giguère C A, Dall'Aglio A, McQuinn M, Fechner C, Zaldarriaga M, Hernquist L and Dutta S 2010 *Astroph. J.* **718** 199–230
[22] Faucher-Giguère C A, Lidz A, Hernquist L and Zaldarriaga M 2008 *Astroph. J.* **688** 85-107
[23] Becker G D and Bolton J S 2013 *MNRAS* **436** 1023–39
[24] Khaire V and Srianand R 2019 *MNRAS* **484** 4174–99
[25] Hiss H, Walther M, Oñorbe J and Hennawi J F 2019 *Astroph. J.* **876** 71
[26] Puchwein E, Haardt F, Haehnelt M G and Madau P 2019 *MNRAS* **485** 47–68
[27] Upton Sanderbeck P and Bird S 2020 *MNRAS* **496** 4372–4382